

Ab initio vibrationalrotational spectrum of potassium cyanide: KCN. II. Large amplitude motions and rovibrational coupling

Jonathan Tennyson and Ad van der Avoird

Citation: *J. Chem. Phys.* **76**, 5710 (1982); doi: 10.1063/1.442966

View online: <http://dx.doi.org/10.1063/1.442966>

View Table of Contents: <http://jcp.aip.org/resource/1/JCPSA6/v76/i12>

Published by the [American Institute of Physics](#).

Additional information on *J. Chem. Phys.*

Journal Homepage: <http://jcp.aip.org/>

Journal Information: http://jcp.aip.org/about/about_the_journal

Top downloads: http://jcp.aip.org/features/most_downloaded

Information for Authors: <http://jcp.aip.org/authors>

ADVERTISEMENT



Goodfellow
metals • ceramics • polymers • composites
70,000 products
450 different materials
small quantities fast

www.goodfellowusa.com

***Ab initio* vibrational-rotational spectrum of potassium cyanide: KCN. II. Large amplitude motions and rovibrational coupling**

Jonathan Tennyson and Ad van der Avoird

Instituut voor Theoretische Chemie, Universiteit Nijmegen, Toernooiveld, Nijmegen, The Netherlands

(Received 29 January 1982; accepted 17 February 1982)

The ten lowest vibrational states of KCN have been obtained *ab initio* using the close-coupling method of Le Roy and Van Kranendonk. Fundamental vibrations are found to lie at 114.7 (bending) and 293.0 cm^{-1} (K-CN stretch). Comparison is made with previous results obtained using the Watson Hamiltonian for nonlinear molecules and separating the rotations and vibrations. It is found that this model breaks down for the higher librations near and above the barrier to inversion. For these states the average geometry of the KCN molecule shifts towards the linear isocyanide (KNC) structure. Properties of the vibrational states and the rotational spectrum are analyzed.

I. INTRODUCTION

Recent experimental work on the rotational spectrum of potassium cyanide (KCN) has shown it to have a triangular structure,^{1,2} a result confirmed by *ab initio* calculations.^{3,4} Furthermore, these *ab initio* calculations showed there to be a low barrier ($\sim 500 \text{ cm}^{-1}$) to inversion at the isocyanide geometry. While one can expect a few vibrational states to be confined below this barrier, states which undergo large amplitude vibrations across the barrier should be appreciably populated at moderate vibrational temperatures. The microwave experiments were conducted at 1150 K. In these experiments rotational transitions from at least 11 vibrational states have been observed,² although only those from the ground state have been definitely assigned.

In contrast to the rotational spectrum, there is little experimental data on the gas phase vibrational spectrum of KCN. The only direct measurement⁵ observed just one transition (at 207 cm^{-1}) between 200 cm^{-1} and the C-N stretch at 2158 cm^{-1} . An estimate of the inertial defect from the ground state rotational spectrum placed the bending mode ω_2 at $\sim 157 \text{ cm}^{-1}$.² This is in fair agreement with the matrix isolation study of Ismail *et al.*⁶ who found the K-CN stretch ω_1 at 288 cm^{-1} , the bending mode ω_2 at 139 cm^{-1} , and the CN stretch ω_3 at 2050 cm^{-1} .

In a recent paper,⁷ henceforth referred to as I, Tennyson and Sutcliffe predicted that the fundamentals ω_1 and ω_2 lie at 303 and 120 cm^{-1} , respectively. In that work they solved Watson's form of the Hamiltonian⁸ using the method of Whitehead and Handy.⁹ In this approach the problem is expressed in normal coordinates expanded about some equilibrium structure. This allows an optimal separation of vibrational and rotational motions, which is only valid in the limit of small amplitude vibrations. Use of this separation gave good results for the low lying vibrational states of KCN. This allowed tentative assignments to vibrational levels to be made for the observed rotational spectrum of the vibrational excited states.

Of particular interest in KCN is the nature of the vi-

brational states below, at, and above the barrier to inversion. For LiCN, states in which the Li^+ ion moves nearly freely about the CN^- ion (leading to a "polytopic" bond¹⁰) have been predicted to predominate in the gas phase.¹⁰ For KCN, there is probably a transition from low-lying localized librational states to higher hindered internal rotations, comparable in nature to the orientational order-disorder phase transition observed in alkali cyanide crystals¹¹ (including KCN).

For the higher bending vibrational states near and above the barrier, which should behave like hindered internal rotors, one can expect the separation between vibrations and rotations, that is always used in practice with Watson's Hamiltonian, to break down. Moreover, the Watson Hamiltonian for a nonlinear molecule⁸ does not allow for the linear geometries which occur at the barrier, meaning that any method based on this Hamiltonian cannot be expected to perform well for states with significant amplitudes at the barrier.

In this paper, we solve the nuclear dynamics problem for KCN making no assumptions about the separability of the rotational and vibrational Hamiltonian. This is done using the method of Le Roy and Van Kranendonk,¹² which sets up a secular problem within the close-coupling formalism. It uses analytic integrals over a basis of spherical harmonics (free rotor functions) in the bending mode, which are coupled to the overall rotation. This basis should give a better representation of the hindered rotations or large amplitude librations which lie above the barrier.

The method has been successfully used to calculate the spectra of van der Waals molecules, especially H_2 -rare gas complexes,¹² where the near isotropic potentials allow almost free rotations in the bending coordinate. The method has recently been reviewed by Le Roy and Carley.¹³ Carney *et al.*¹⁴ have reviewed variational methods for the nuclear dynamics problem.

A related method by Shapiro and Balint-Kurti,¹⁵ formulated in body fixed coordinates, has been used to obtain the rovibrational spectrum of water with good results. Although the barrier to linearity in water is over 12 000 cm^{-1} ,¹⁶ expansion of the highly localized

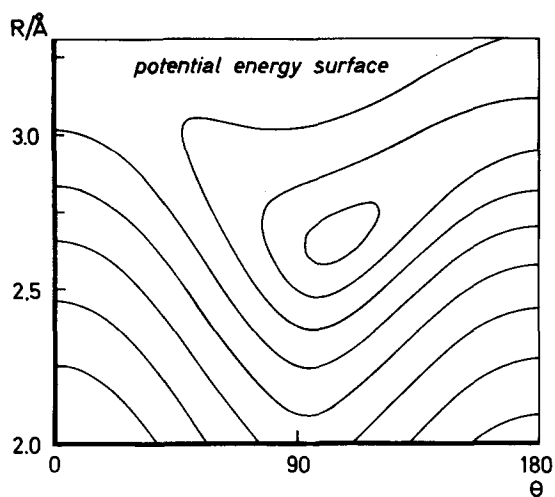


FIG. 1. Potential energy surface for KCN as calculated by Wormer and Tennyson (Ref. 3). R is the distance from the CN center of mass to K, and θ the angle R makes with $r(\text{CN})$; $\theta = 0$ for KCN. Starting from the closed contour, the contours lie at $-38\,964.4$, $-38\,419.4$, $-37\,321.8$, $-35\,126.4$, $-30\,735.6$, $-21\,954.0$, -4390.8 , and $30\,735.6$ cm^{-1} .

vibrational states with free rotor functions showed convergence with about ten functions.¹⁵ This suggests that for the comparatively “floppy” KCN, free rotor functions should provide a satisfactory expansion even for the more localized vibrational states below the barrier. Recently, Kidd, Balint-Kurti, and Shapiro¹⁷ have used hindered rotor functions to give a faster convergent basis set for water. Although functions of this type should give a better representation of the low lying states in KCN, the same set of hindered rotor functions would not necessarily be appropriate for the states lying above the barrier. Therefore, we have not used them.

By solving the nuclear dynamics problem for KCN over a range of vibrational states, we hope to gain insight into the behavior of the molecule as the amplitude of its motion increases. Furthermore, comparison with paper I allows an assessment to be made of two very different methods for the dynamical problem. In particular, it is possible to check the low lying states obtained using the method of Whitehead and Handy⁹ and find where their method ceases to be appropriate.

II. POTENTIAL SURFACE

In this paper, as in I, we use the analytic KCN surface fitted by Wormer and Tennyson³ to their extended basis SCF calculations. This surface is only two dimensional as the CN bond length r was frozen at its SCF optimized value 1.157 Å. Exploratory calculations by both Wormer and Tennyson³ and Klein *et al.*⁴ found little coupling in the potential between r and the other coordinates. Furthermore, the CN stretch, which lies in the region of 2100 cm^{-1} ,^{5,6} is well separated from the other fundamental energies. This suggests that treating the CN as a rigid rotor should not lead to too great a loss of accuracy and allows the Wormer-Tennyson potential to be used in its original form

$$V(R, r_\theta, \theta) = \sum_{\lambda=0}^8 P_\lambda(\cos \theta) V_\lambda(R), \quad (1)$$

where $\mathbf{R} = (R, \hat{R})$ is the vector from the CN center of mass to the K nucleus and θ the angle \mathbf{R} makes with the vector \mathbf{r} (the CN axis) measured from C. The coefficients of the Legendre polynomial expansion as functions of R are given by Wormer and Tennyson.³ Figure 1 shows the potential in the region of the minimum. We note that the geometry at the minimum is indeed triangular, although the barrier to inversion through the linear isocyanide (KNC) structure is only 503.9 cm^{-1} . The barrier through the linear cyanide (KCN) structure is considerably larger. Finally, we note that the SCF optimized CN bond length is slightly shorter than that obtained from experiment² or when extensive configuration interaction is used.¹⁸

III. METHOD

As the second step in the Born-Oppenheimer approximation, the Hamiltonian for the atom-rigid diatom nuclear problem can be written, after separating out the center of mass motion, as

$$H(\mathbf{R}, \mathbf{r}) = -\frac{\hbar^2}{2\mu R} \left(\frac{\partial^2}{\partial R^2} \right) R + \frac{1^2}{2\mu R^2} + \frac{j^2}{2\mu_d r_f^2} + V(R, r_f, \theta) \quad (2)$$

in “space-fixed” coordinates.¹² In Eq. (2), μ equals $m_a m_d / (m_a + m_d)$, with m_a and m_d being the atomic and diatomic masses, respectively; μ_d is the reduced mass of the diatom. The diatom is assumed to have a fixed bond length r_f . The eigenfunctions of the operators l^2 and j^2 are spherical harmonics in the angles \hat{R} and \hat{r} , respectively.

Within the zero-coupling limit, i.e., if $V(R, r_f, \theta) = V(R)$, Eq. (2) becomes separable and the eigenfunctions can be written as $[R^{-1} \chi_{nl}(R)] \mathcal{Y}_{ji}^{JM}(\hat{\mathbf{R}}, \hat{\mathbf{r}})$. χ_{nl} are the solutions of the pseudodiatomic Schrödinger equation

$$\left[-\frac{\hbar^2}{2\mu} \frac{d^2}{dR^2} + l(l+1) \frac{\hbar^2}{2\mu R^2} + V(R) - E_0(n, l) \right] \chi_{nl}(R) = 0 \quad (3)$$

and the total angular momentum eigenfunction \mathcal{Y}_{ji}^{JM} is defined as

$$\mathcal{Y}_{ji}^{JM}(\hat{\mathbf{R}}, \mathbf{r}) = \sum_{m=-j}^j (J, M | j, m; l, M-m) Y_{jm}(\mathbf{r}) Y_{l, M-m}(\hat{\mathbf{R}}), \quad (4)$$

where $(J, M | j, m; l, M-m)$ is a Clebsch-Gordan coefficient.¹⁹

Solutions of the full Schrödinger equation for the problem

$$[H(\mathbf{R}, \mathbf{r}) - E_\alpha^J] \Psi_\alpha^{JM} = 0 \quad (5)$$

can be obtained in a basis of zero-coupling functions giving

$$\Psi_\alpha^{JM}(\mathbf{R}, \mathbf{r}) = R^{-1} \sum_j \sum_i \mathcal{Y}_{ji}^{JM}(\hat{\mathbf{R}}, \hat{\mathbf{r}}) G_{ji}^{J\alpha}(R), \quad (6)$$

where

$$G_{ji}^{J\alpha} = \sum_n a_{nji}^{J\alpha} \chi_{ni}(R) \quad (7)$$

and $\mathbf{a}^{J\alpha}$ is the vector of expansion coefficients for the α th state with total rotational quantum number J .

$$\left\{ \frac{\hbar^2}{2\mu} \left[\frac{-d^2}{dR^2} + \frac{l'(l'+1)}{R^2} \right] + \frac{j'(j'+1)\hbar^2}{2\mu_d r_f^2} - E_\alpha^J \right\} G_{ji}^{J\alpha} + \sum_{j''} \sum_{l''} \sum_{\lambda} f_{\lambda}(j', l'; j'', l''; J) V_{\lambda}(R) G_{j''l''}^{J\alpha} = 0, \quad (8)$$

where it has been assumed that the potential is expressed as the Legendre expansion of Eq. (1). This allows the angular integration over the potential to be performed analytically giving

$$f_{\lambda}(j', l'; j'', l''; J) = (-1)^{j''+l''+J} [(2j'+1)(2j''+1)(2l'+1)(2l''+1)]^{1/2} \begin{pmatrix} j'' & \lambda & j' \\ 0 & 0 & 0 \end{pmatrix} \begin{pmatrix} l'' & \lambda & l' \\ 0 & 0 & 0 \end{pmatrix} \begin{Bmatrix} J & l' & j' \\ \lambda & j'' & l'' \end{Bmatrix}, \quad (9)$$

as first shown by Percival and Seaton.²¹ The symmetry of f_{λ} forces it to be zero unless $j''+\lambda+j'$ and $l''+\lambda+l'$ are both even. This causes the secular equations, which are obtained from Eq. (8) by substituting Eq. (7) and integrating, and which are already blocked by J , to be further block factorized according to whether $j'-l'$ is odd or even.

The method of Le Roy and Van Kranendonk¹² uses numerical radial basis functions $\chi_{ni}(R)$. These are obtained by the explicit numerical solution of Eq. (3). In principle, a complete set of radial basis functions may be obtained for only one value of l , l_{ref} , and it is convenient to work with a basis generated in this fashion as it is orthogonal. In the case of KCN, the radial potential is sufficiently deep for $\chi_{ni}(R)$ to only weakly depend on l ; we, therefore, worked entirely with $l_{\text{ref}}=0$ and henceforth, will drop the second index on χ_{ni} . Furthermore, the radial potential supports several hundred bound states and so there is no need to include functions from the continuum as is necessary for shallower potentials.²²

In their work, Le Roy and Van Kranendonk¹² set the potential $V(R)$ in Eq. (3) equal to $V_0(R)$, the isotropic potential and first term in an expansion like that of Eq. (1). Preliminary calculations showed only slow convergence with a radial basis generated in this manner. The main problem is that the minimum of $V_0(R)$ lies at larger R , 2.891 Å, than the equilibrium geometry of Wormer and Tennyson,³ $R_e = 2.675$ Å. Instead, a cut through the potential at the equilibrium angle $\theta_e = 105.7^\circ$ was used, giving $V(R) = V(R, \theta_e, r_e)$. The resulting basis was found to give considerably more rapid convergence.

IV. CALCULATIONS WITH $J = 0$

The basis sets outlined in the previous sections are essentially two dimensional within a given rotational state (J, M), i. e., the size of the secular problem increases linearly with both the number of radial functions χ_n and angular functions \mathcal{Y}_{ji}^{JM} included in the basis. For our results to be satisfactorily converged, it is necessary to consider increases in the basis with both these sets.

Table I shows the effect of increasing the number of radial basis functions. All $\chi_n(R)$ were included from

Substituting Eqs. (2) and (6) into Eq. (5), multiplying from the left by $\mathcal{Y}_{ji}^{JM}(\hat{R}, \hat{r})^*$ and integrating over all variables except R yields the so called close-coupled equations, originally derived for scattering problems by Arthurs and Dalgarno,²⁰

$n=0$ to n_{max} , so that the final basis set was made up using $n_{\text{max}}+1$ radial functions. These functions were generated by numerically solving Eq. (3) for a grid of 1200 points until E_0 had converged to within 0.05 cm^{-1} . The radial wave functions were found to be insensitive to either increasing the grid or lowering the convergence threshold. It is clear from Table I that the radial basis set is very well saturated with $n_{\text{max}}=11$ (12 functions), and we took this value for all further calculations.

It is not so easy to generate angular basis sets in such a uniform manner. This is because the ranges of the summations over j and l in Eq. (6) are linked; they depend on J via the triangular relationships inherent in the Clebsch-Gordan coefficient of Eq. (4). We followed the usual practice^{12-15, 17} and included in our basis all possible angular functions which had j less than or equal to some j_{max} . Table II shows the convergence of the lowest ten states with $J=0$ and increasing j_{max} .

It is clear from Table II that convergence is considerably slower for the angular functions than for the radial problem. Indeed, twice as many angular functions (a total of $j_{\text{max}}+1$ for $J=0$) are needed to give convergence similar to that found with $n_{\text{max}}=11$. Even for $J=0$, it was no longer possible for us to retain the whole secular matrix in the computer main store for

TABLE I. Convergence of ground state energy (in cm^{-1}) and lowest nine band origins (in cm^{-1}) with radial basis set. All calculations are for $J=0$ and $j_{\text{max}}=15$.

	n_{max}		
	10	11	12
Ground state	-38 861.166 ^a	-38 861.166 ^a	-38 861.166 ^a
Band origin			
1	117.84	117.84	117.84
2	221.21	222.21	222.21
3	297.21	297.21	297.21
4	319.67	319.67	319.67
5	394.75	394.73	394.73
6	425.96	425.94	425.94
7	464.76	464.42	464.41
8	528.69	528.50	528.48
9	542.33	541.95	541.92

^aEnergy relative to dissociated K^+ and CN^- .

TABLE II. Convergence of ground state energy (in cm^{-1}) and lowest nine band origins (in cm^{-1}) with angular basis set. All calculations are for $J=0$ and $n_{\text{max}}=11$.

		j_{max}				
		15	18	19	22	23
Ground state		-38 861.166	-38 861.373	-38 861.391	-38 861.396	-38 861.397
Band origin	1	117.84	116.21	116.15	116.10	116.09
	2	222.21	218.25	218.11	217.79	217.78
	3	297.21	295.08	294.56	294.30	294.29
	4	319.67	315.50	314.97	314.59	314.58
	5	394.73	382.93	380.59	379.64	379.56
	6	425.94	421.26	421.12	420.51	420.45
	7	464.42	451.38	449.57	448.53	448.42
	8	528.50	500.36	499.44	495.23	494.90
	9	541.95	532.92	531.43	530.43	530.40

these high values of j_{max} . We were thus forced to use a method of iterative diagonalization^{23,24} and to obtain only the lowest (usually ten) eigenvalues. As the secular matrix was not, in general, diagonally dominant, convergence of this diagonalization was slow. However, in some cases, such as in basis set optimization, a good initial guess to the eigenvectors could be provided by a previous calculation.

For $J=0$, the states essentially correspond to the vibrational levels obtained in paper I. Table II thus shows the convergence of the vibrational spectrum with angular basis. The rotational spectrum will not necessarily exhibit the same properties. The size of the secular problem grows linearly with the total rotational quantum number J , and thus the level of accuracy that can be attained in the calculations decreases with increasing J .

Table III shows the effect of varying the CN bond length. Compared are results for the SCF optimized bond length $r_e = 1.57 \text{ \AA}$ and the best experimental estimate of the vibrationally averaged bond length $r_0 = 1.71 \text{ \AA}$ from isotopic substitution.²⁵ Clearly, the longer CN bond length lowers the energy of all states. This is because the effect of lengthening is to reduce the separation between rotational states of the CN diatom. As the experimental CN distance is more realistic than that of Wormer and Tennyson, the vibrational spectrum calculated for $r_0 = 1.171 \text{ \AA}$ represents our best estimate.

Analysis of our wave function (see Fig. 2) suggests that the first and third excited states are the bending (ω_2) and K-CN stretching (ω_1) fundamentals, the second excited state being a bending overtone. Our stretch at 293.0 cm^{-1} is thus in surprisingly good agreement with the matrix isolation value of Ismail *et al.*,⁶ 288 cm^{-1} , but our bending fundamental at 114.7 cm^{-1} lies 25 cm^{-1} lower than theirs. As suggested in I, the transition observed at 207 cm^{-1} by Leroi and Klemperer⁵ could well be the bending overtone.

Table III also compares our results to those obtained in I, using the method of Whitehead and Handy.⁹ In order to compare absolute energies, it is necessary to make allowances for the CN stretch zero-point ener-

gy, which does not enter the present calculations as the CN is treated as rigid. In paper I, a full vibrational problem was solved and the appropriate CN zero-point energy was found to be 1064.9 cm^{-1} . Including this shows the previous ground state to be lower in energy and thus in a variational sense better represented.

However, the excited states of paper I lie higher in energy than those calculated using the method of Le Roy and Van Kranendonk.¹² This leads to slightly larger values for the fundamental transitions, namely, 119.7 and 302.7 cm^{-1} , compared with 116.1 and 294.3 cm^{-1} found with the same CN bond length in the current study. This discrepancy is small and the two methods are clearly in good agreement for these low lying states.

The same cannot be said for the higher vibrational states. There is serious disagreement between the two calculations for the fourth excited and higher states, with the previous calculations in paper I overestimating all the transition energies. This suggests that the higher states in I, although variationally correct, have little physical significance and it could be argued that the results of paper I systematically omit certain vibrational states.

TABLE III. Comparison of the ground state energies (in cm^{-1}) and $J=0$ vibrational spectrum (in cm^{-1}) for this work ($j_{\text{max}}=23$) and paper I. Also shown is the difference between SCF optimized and experimental CN bond lengths r .

		This work	This work	Paper I
$r/\text{\AA}$		1.171	1.157	1.157
Ground state energy		-38 862.41	-38 861.40	-38 863.2 ^a
Band origin	1	114.7	116.1	119.7
	2	215.4	217.8	241.9
	3	293.0	294.3	302.7
	4	312.5	314.6	382.9
	5	376.5	379.6	438.6
	6	418.4	420.5	524.0
	7	445.4	448.4	588.3
	8	490.7	494.9	616.7
	9	526.7	530.4	

^aCorrected for 1064.9 cm^{-1} zero-point energy for the CN stretch.

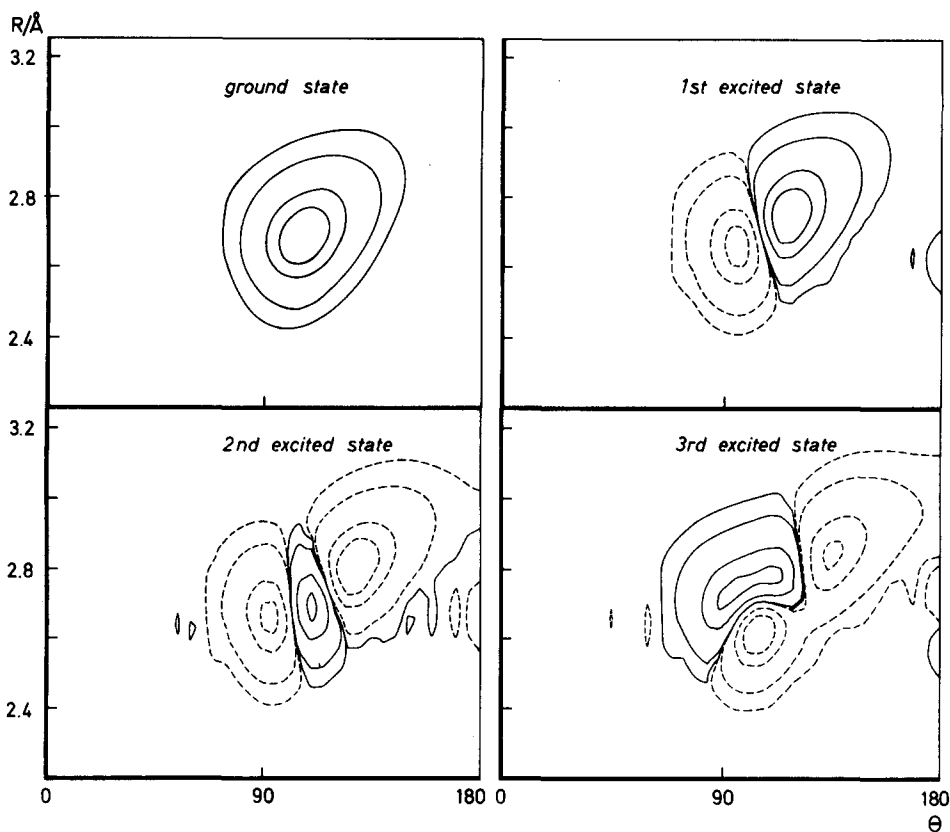


FIG. 2. The lowest four vibrational wave functions computed with $J=0$. The contours link points where the wave function has 0.3%, 3%, 30%, and 60% of its maximum amplitude. Solid curves enclose regions of positive amplitude and dashed curves regions of negative amplitude.

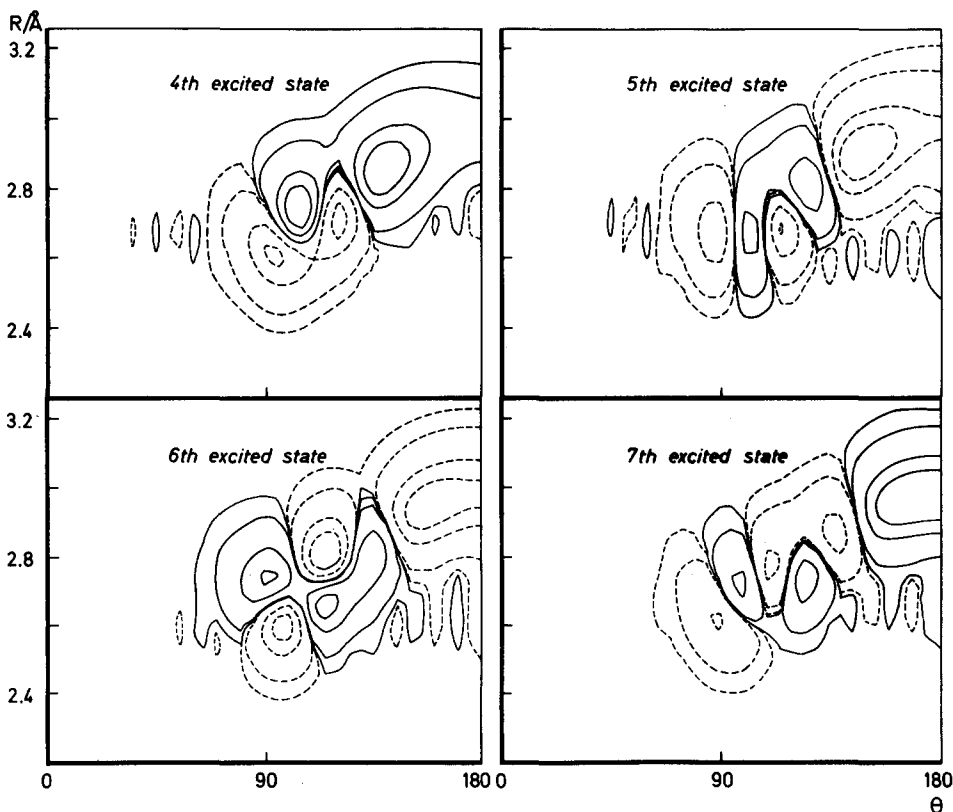


FIG. 3. Vibrational wave functions computed for $J=0$ with energies in the region of the barrier. Contours are as for Fig. 2.

TABLE IV. Vibrationally averaged geometric parameters for the $J=0$ state of the ten lowest vibrational levels.

	$\arccos(\langle \cos \theta \rangle)$ (deg)	$\arccos(\langle \cos^2 \theta \rangle^{1/2}) - \arccos(\langle \cos \theta \rangle)$ (deg)	$\langle R^{-2} \rangle^{-1/2}$ (Å)
Ground state	106.4	1.3	2.689
1st excited state	110.4	3.5	2.718
2nd	114.5	5.1	2.749
3rd	109.1	5.2	2.723
4th	115.5	5.6	2.757
5th	123.8	7.5	2.817
6th	115.5	6.9	2.765
7th	129.1	7.4	2.847
8th	125.1	9.4	2.836
9th	118.1	7.8	2.786
Equilibrium values	105.7	...	2.675

Figures 2 and 3 show plots of the lowest eight vibrational states of KCN obtained by numerically evaluating our wave functions at a grid of points which can then be linked to give contours. The lowest states, depicted in Fig. 2, are clearly localized about the KCN equilibrium structure. They are even harmonic in appearance. Thus, it is not surprising that for these states the two methods are in fair agreement.

Figure 3 shows the next four vibrational states. These states are more delocalized, showing an increasing density in the region of the barrier at the linear isocyanide structure. It is for this structure that Watson's Hamiltonian for nonlinear molecules⁸ is not valid and, hence, the method of Whitehead and Handy⁹ breaks down.

The minimum in Wormer and Tennyson's surface³ lies at $-39\,086.1\text{ cm}^{-1}$ (relative to dissociated K^+ and CN^-). Because of zero-point energy considerations, it is difficult to say which is the first state that lies above the inversion barrier. If the zero-point energy of the stretching fundamental is assumed constant at 145.6 cm^{-1} , then the seventh excited state lies 18 cm^{-1} above the barrier. However, inspection of the curvature of the surface at the barrier suggests a stretching zero point energy of $\sim 166\text{ cm}^{-1}$. This would make the eighth excited state the first one above the barrier.

What is clear from Fig. 3, however, is that states which lie below the barrier (by up to 70 cm^{-1}) show appreciable density in the classically forbidden region around the barrier. The Whitehead-Handy method thus breaks down not just for states which lie above the barrier, but also for those which show appreciable tunneling. This raises the problem of deciding when this tunneling is significant for a "floppy" molecule. In this context we mention the recent work of Bartholomae, Martin, and Sutcliffe²⁶ who, using the Whitehead-Handy method, explicitly constructed a basis set for CH_2^+ which could not probe linear geometries. There is a danger in such an approach that, while variationally

correct results can be so obtained, they may have little significance as the wave function is constrained to be small in physically significant regions of the surface.

In Table IV we present some vibrationally averaged geometric parameters for the lowest ten vibrational states. It is clear that, in general, both the average value of θ and the amplitude of vibration increases with vibrational excitation. This results in states which no longer vibrate about the equilibrium geometry but about some more linear structure. The vibrationally averaged value of R also increases with vibrational excitation. This is because the minimum in the potential with respect to R lies at larger R values as θ tends to 180° , as shown in Fig. 1.

V. ROTATIONAL EXCITATIONS

Table V gives calculated rotational levels for the vibrational ground state. These values are obtained by performing a complete vibration-rotation calculation for a total angular momentum J and taking the energies relative to the lowest level in a $J=0$ calculation. For $J > 0$, the calculations are performed in two separate pieces according to whether odd (o) or even (e) combinations $j-l$ contribute. The eigenvalues in Table V have been labeled accordingly.

It is clear that to within the convergence of our angular basis [$\sim 0.005\text{ cm}^{-1}$ for $j_{\text{max}}=19$ (see Table V)] there is excellent agreement between the rotational spectra obtained using the methods of Le Roy and Van Kranendonk, and Whitehead and Handy. This demonstrates that, for the ground state at least, the separation between vibrational and rotational problems works extremely well. In paper I, use of this separation allowed rotational states up to $J=25$ to be calculated in only a few seconds computer time. Without this separation, the size of the secular problem makes calculations with $J > 4$ prohibitively expensive. This is because, although secular matrices with dimensions of order 700 are not large by comparison with today's

TABLE V. Rotational levels of the vibrational ground state (in cm^{-1}) compared with previous results (Ref. 7) and experiment (Refs. 2 and 25). The results for a J state are given relative to $J=0$ and divided into "even" and "odd" ($j-l$) blocks (see Sec. III). All calculations are for $r=1.157 \text{ \AA}$.

J		$j_{\max}=18$	$j_{\max}=19$	Paper I	Expt.
0		-38 861.3732	-38 861.3910	-38 863.2	
1	e	2.3429	2.3544	2.3277	2.0933
	o	0.2877	0.2877	0.2879	0.3158
2	e	2.3328	2.3449	2.3377	2.1068
	o	0.8631	0.8630	0.8636	0.9378
3	e	2.8980	2.9100	2.9234	2.7523
	o	9.0342	9.0319	9.0430	8.0839
4	e	2.9283	2.9405	2.8934	2.7115
	o	9.0341	9.0319	9.0430	8.0838
5	e	3.8064		3.7421	3.6387
	o	9.8970		9.9068	9.0310
6	e	20.1009		20.1308	17.9496
	o	1.7261		1.7271	1.8943
7	e	3.7460		3.8020	3.7195
	o	9.8972		9.9066	9.0315
8	e	20.1008		20.1308	17.9496
	o	2.8762		2.8782	3.1573
9	e	4.8762		4.9735	5.0096
	o	11.0479		11.0581	10.2950
10	e	21.2510		21.2823	19.2122
	o	35.5287		35.5961	31.6946
11	e	4.9772		4.8736	4.8746
	o	11.0475		11.0586	10.2936
12	e	21.2512		21.2824	19.2122
	o	35.5289		35.5961	31.6946

configuration interaction calculations, these matrices are not diagonally dominant and have few zero elements. Furthermore, it is necessary to obtain at least the $J+1$ lowest eigenvalues. This combines to make the iterative diagonalization procedure^{23,24} only slowly convergent.

Table V shows that the calculated and experimental rotational spectra only agree to within 10%. This problem was discussed at length in paper I. It is associated with inaccuracies in the *ab initio* potential energy surface. In particular, the equilibrium structure obtained by Wormer and Tennyson³ differs by 4% in R , 8% in θ , and 1.2% in r from the best experimental values.²⁵ This was found to be the major cause of the discrepancy. Changing the CN value to the experimental value should improve the agreement of certain transitions, in particular, the so called *b*-type transitions,²⁷ but would not change the discrepancy in most of the calculated transitions.

It is interesting to know how the rotational spectrum of KCN changes with vibrational state, especially in view of the shifts in average geometry shown in Table IV. Table VI shows the $J=0 \rightarrow 1$ (e) transition for the lowest ten vibrational states. The transition energies are shown for several levels of calculation, as it is clear that for the higher vibrational states our angular basis set is not completely saturated. The oscillations found for some states are indicative of the fact that increasing j_{\max} alternately stabilizes the $J=0$ and $J=1$ states. The results are, however, sufficiently well

converged for trends in the transitions to become apparent.

Inspection of Table VI shows that the rotational transitions fall roughly into three groups. In the first group, comprising the ground and first four excited vibrational states, the dependence of the rotational splitting on vibrational level is small. This is typical of a molecule undergoing small amplitude vibrations.

For the fifth and sixth vibrationally excited states, the $J=0 \rightarrow 1$ (e) splitting is about twice that found for the lower vibrational states. These states mark the onset of tunneling through the barrier, and as shown in Table IV and Fig. 3, they are no longer vibrating about the minimum in the potential energy surface.

Finally, states above and including the seventh vibrationally excited state show very large $J=0 \rightarrow 1$ (e) splittings. The seventh excited state lies at about the top of the barrier, and thus these higher states are the ones which undergo hindered rotations across the barrier. At the barrier the molecule is linear which causes the moment of inertia in the linear direction to be zero. The trends shown in Table VI for the $J=0 \rightarrow 1$ (e) transition are thus explained by increasing linearity with vibrational excitation. For the large amplitude vibrational states, it is not possible to use a rovibrational separation and, hence, no comparison can be drawn with rotational spectra obtained using the method of paper I.

TABLE VI. $J=0 \rightarrow 1$ (e) transition energies (in cm^{-1}) for the lowest ten vibrational states as a function of increasing angular basis set. For vibrational spacings see Table III.

	j_{max}					
	18	19	20	21	22	23
Ground state	2.343	2.354	2.350	2.352	2.351	2.351
1st Excited state	2.600	2.566	2.562	2.569	2.564	2.570
2nd	3.252	2.850	3.043	2.961	2.987	2.980
3rd	2.510	2.901	2.787	2.808	2.819	2.810
4th	3.367	3.477	3.513	3.417	3.462	3.437
5th	5.225	6.962	5.760	6.209	6.019	6.049
6th	5.640	5.111	5.744	5.440	5.456	5.486
7th	16.78	16.71	14.78	15.09	14.62	14.67
8th	20.75	17.07	19.64	18.75	19.01	19.00
9th	22.61	20.15	19.44	19.23	18.95	18.93

VI. CONCLUSIONS

In this study, we have performed calculations for the lowest ten vibrational states of KCN. While we obtain good agreement with previous⁷ results for localized states lying around the potential minimum in KCN, we have found that the method of Whitehead and Handy⁹ fails for higher states, even some of those which lie below the barrier to inversion at the linear isocyanide geometry. For these intermediate states, tunneling is found to be significant. Comparison of rotational spectra shows that for the ground state separation of the rotational and vibrational problems introduces no significant error.

Analysis of our higher vibrational states shows that KCN undergoes large amplitude bending vibrations (librations or hindered rotations) which are no longer centered at the equilibrium structure. KCN thus effectively moves towards an isocyanide structure in its vibrationally excited states. This is reflected in the calculated rotational spectra of these states, which show large changes from those calculated for the ground state. It would be interesting to see whether these shifts in the rotational spectrum can be observed experimentally.

Finally, Wormer and Tennyson³ noted that their SCF calculated dipole moment could be well represented by long range theory: by considering the ions K^+ and CN^- and their polarizabilities. This should allow a dipole surface for KCN to be easily fitted. With this and the wave functions presented here, vibrationally averaged dipole moments for each state and transition dipoles (giving infrared intensities) could be calculated. As KCN undergoes large amplitude vibrations, especially in its vibrationally excited states, one would expect its dipole to be significantly different from that given for the minimum energy geometry by Wormer and Tennyson.

ACKNOWLEDGMENTS

We wish to thank Professor R. J. Le Roy for making available a copy of the program written by himself and

J. E. Grabenstetter. We would also like to thank Dr. J. J. van Vaals and Dr. W. L. Meerts for helpful discussions and for communicating their results prior to publication. We are grateful to Dr. J. Vliegthart for supplying some test results. Finally, many fruitful discussions with Dr. B. T. Sutcliffe are acknowledged.

- ¹P. Kuijpers, T. Törring and A. Dymanus, *Chem. Phys. Lett.* **42**, 423 (1976).
- ²T. Törring, J. P. Bekooy, W. L. Meerts, J. Hoeft, E. Tie-mann, and A. Dymanus, *J. Chem. Phys.* **73**, 4875 (1980).
- ³P. E. S. Wormer and J. Tennyson, *J. Chem. Phys.* **75**, 1245 (1981).
- ⁴M. L. Klein, J. D. Goddard, and D. G. Bounds, *J. Chem. Phys.* **75**, 3909 (1981).
- ⁵G. E. Leroi and W. Klemperer, *J. Chem. Phys.* **35**, 774 (1961).
- ⁶Z. K. Ismail, R. H. Hauge, and J. L. Margrave, *J. Chem. Phys.* **57**, 5137 (1972); *J. Mol. Spectrosc.* **54**, 402 (1975).
- ⁷J. Tennyson and B. T. Sutcliffe, *Mol. Phys.* (in press).
- ⁸J. K. G. Watson, *Mol. Phys.* **15**, 479 (1968).
- ⁹R. J. Whitehead and N. C. Handy, *J. Mol. Spectrosc.* **55**, 356 (1975).
- ¹⁰E. Clementi, H. Kistenmacher, and H. Popkie, *J. Chem. Phys.* **70**, 4481 (1979).
- ¹¹For example, see M. Klein and I. R. McDonald, *Chem. Phys. Lett.* **78**, 383 (1981).
- ¹²R. J. Le Roy and J. van Kranendonk, *J. Chem. Phys.* **61**, 4750 (1974).
- ¹³R. J. Le Roy and J. S. Carley, *Adv. Chem. Phys.* **42**, 353 (1980).
- ¹⁴G. D. Carney, L. L. Sprandel, and C. W. Kern, *Adv. Chem. Phys.* **37**, 305 (1978).
- ¹⁵M. Shapiro and G. G. Balint-Kurti, *J. Chem. Phys.* **71**, 1461 (1979).
- ¹⁶Ch. V. S. Ramachandra Rao, *J. Mol. Spectrosc.* **89**, 197 (1981).
- ¹⁷I. F. Kidd, G. G. Balint-Kurti, and M. Shapiro, *Faraday Discuss. Chem. Soc.* **71**, 287 (1981).
- ¹⁸P. R. Taylor, G. B. Bacskay, N. S. Hush, and N. C. Hurley, *J. Chem. Phys.* **70**, 4481 (1979).
- ¹⁹See, for example, D. M. Brink and G. T. Satchler, *Angular Momentum*, 2nd ed. (Clarendon, Oxford, 1968).
- ²⁰A. M. Arthurs and A. Dalgarno, *Proc. R. Soc. London Ser. A* **256**, 540 (1960).

- ²¹I. C. Percival and M. J. Seaton, Proc. Cambridge Philos. Soc. **53**, 654 (1957).
- ²²R. J. Le Roy, J. S. Carley, and J. E. Grabenstetter, Faraday Discuss. Chem. Soc. **62**, 169 (1977).
- ²³I. Shavitt, C. F. Bender, A. Pipano, and R. P. Hosteny, J. Comput. Phys. **11**, 90 (1973).
- ²⁴R. C. Raffanetti, J. Comput. Phys. **32**, 403 (1979).
- ²⁵J. J. van Vaals and W. L. Meerts (to be published).
- ²⁶R. Bartholomae, P. Martin, and B. T. Sutcliffe, J. Mol. Spectrosc. **87**, 367 (1981).
- ²⁷W. Gordy and R. L. Cook, *Microwave and Molecular Spectra*, 2nd ed. (Interscience-Wiley, New York, 1970), Chap. 7.